Physical modeling of 3-D turbulence wind field for floating offshore wind turbines

Zenghui Liu
Ph.D Student, College of Civil Engineering, Tongji University, Shanghai, P.R. China

Jianbing Chen*
University Distinguished Professor. College of Civil Engineering, Tongji University, Shanghai, P.R. China

Yongbo Peng
Shanghai Institute of Disaster Prevention and Relief, Tongji University, Shanghai, 200092, P.R China

Jie Li
Shanghai Institute of Disaster Prevention and Relief, Tongji University, Shanghai, 200092, P.R China

ABSTRACT: Wind load is one of the most important dynamic excitations of floating offshore wind turbine (FOWT) systems. Reasonable description and simulation of turbulence wind field lays a significant foundation for the elaborative dynamic response analysis and reliability assessment of FOWTs. In this paper, a physical modeling approach of turbulence wind field for FOWT systems is proposed. The turbulence wind field is regarded as an isotropic homogenous field, and Taylor's frozen hypothesis is adopted to convert the 4-D space-time field into the 3-D spatial field. Then, the wave number spectrum tensor of the isotropic homogenous turbulence field is determined based on the symmetry conditions and the continuity condition of the homogenous turbulence field, and the spectral decomposition technique can thus be employed to represent the 3-D turbulence field. In order to circumvent the obstacle of high-dimensional random variables in the numerical simulation formula, the evolutionary phase model is introduced to represent the random phase angles with just 3 elementary random variables. Using the proposed physical model, a turbulence wind field of 5MW OC3-Hywind floating offshore wind turbine (FOWT) is simulated, and the technique of Fast Fourier Transform (FFT) is adopted to enhance the efficiency of simulation. The numerical results reveal the effectiveness of the proposed approach in the simulation of isotropic homogenous turbulence wind field.

Keywords: Turbulence wind field; Physical modeling; Wind turbine; Evolutionary phase model; Isotropic homogenous field.

The wind load is one of the most significant factors that influence the operating performance and structural safety of the FOWTs. In most current studies of dynamic responses of FOWTs, only one-dimensional wind loads, namely along-wind direction, is considered (Hansen, 2015; Li et al., 2020; Chen et al., 2020). In fact, the atmospheric boundary layer turbulence wind field acting on FOWTs is a typical three-dimensional random field. It is more reasonable that the 3-D turbulence wind field is considered in the dynamic response analysis of FOWTs.

Currently, several modeling approaches for 3-D turbulence wind field have been established, including the Sandia method (Veers, 1984), the Purdue method (Sundar and Sullivan, 1986), and the PNL (Pacific Northwest Laboratory) method (Connell, 1981). The above three approaches were developed based on the spectral representation method (SRM) and the assumption that the three-dimensional turbulence components are independent. Tubino and Solari, (2005) developed a double proper orthogonal decomposition (DPOD) approach based on the principle component model for the simulation of 3-D turbulence wind velocity fields. Different from the above mentioned methods based on SRM, the DPOD approach assumes that the lateral component is uncorrelated to the other two components. Though the above methods have already made pioneering contributions to the simulation of 3-D turbulence wind velocity fields, these methods can not reflect the physical mechanism of the turbulence wind field because they ignore the continuity condition and the governing equation of turbulence. In this view, the physical modeling approaches should be considered. Mann (1998) developed a physical 3-D turbulence wind field based on the rapid distortion theory (RDT) and the homogenous shear turbulence model, and the spectral decomposition technique was adopted to curry out the numerical simulation. However, this approach is quite time-consuming due to the large number of random variables, making the Mann method somewhat inconvenient in practice.

In this paper, a physical modeling approach of 3-D turbulence wind field for FOWT systems is proposed. The turbulence wind field is regarded as an isotropic homogenous field, of which the physical spectrum tensor will be derived. Then the spectral decomposition technique with three dimensional FFT algorithm will be used to generate the numerical wind field. Besides, the evolutionary phase model (Yan and Li, 2011) will be introduced to conquer the high-dimensional random variables challenge that the conventional Monte Carlo methods encountered.

The remaining sections of the paper are arranged as follows: Section 1 introduces some theoretical backgrounds of the physical description of the isotropic homogenous field, Section 2 introduces the proposed modeling approach with the three-dimensional FFT algorithm. In Section 3, a numerical example of a 3-D turbulence wind field acting on the 5-MW FOWT is carried out to illustrate the rationality of the proposed approach, and some conclusions are drawn in Section 4.

1. PHYSICAL DESCRIPTION OF ISOTROPIC HOMOGENOUS FIELD

1.1. Spectral analysis of homogenous field

Define $\mathbf{v}(\mathbf{x},t)=[v_1(\mathbf{x},t),v_2(\mathbf{x},t),v_3(\mathbf{x},t)]$ as the three-dimensional turbulence components at point $\mathbf{x}=(x_1,x_2,x_3)$. For the atmospheric turbulence wind field, the mean wind speed is only height dependent, i.e., $V=V(x_3)$, and can be regarded as a homogenous field. The turbulence components are Gaussian homogenous processes with zero mean values. The cross-correlation function between different components of two points is

$$R_{ij}(\mathbf{x}_1,\mathbf{x}_2,t)=\mathrm{E}\left[v_i(\mathbf{x}_1,t)v_j(\mathbf{x}_2,t)\right]=R_{ij}(\mathbf{r},t) \quad (1)$$

where $\mathbf{r}=\mathbf{x}_1-\mathbf{x}_2$.

According to the Winner-Khintchine formula (Townsend, 1980), the wave-number spectrum and the cross-correlation function of different turbulent components are the Fourier transform pairs, which is

$$\Phi_{ij}(\mathbf{k},t)=\frac{1}{8\pi^3}\int_{R^3}R_{ij}(\mathbf{r},t)\exp(-\mathrm{i}\mathbf{k}\cdot\mathbf{r})\mathrm{d}\mathbf{r} \quad (2)$$

$$R_{ij}(\mathbf{r},t)=\int_{R^3}\Phi_{ij}(\mathbf{k},t)\exp(\mathrm{i}\mathbf{k}\cdot\mathbf{r})\mathrm{d}\mathbf{k} \quad (3)$$

where $\mathrm{d}\mathbf{r}=\mathrm{d}r_1\mathrm{d}r_2\mathrm{d}r_3$, $\mathrm{d}\mathbf{k}=\mathrm{d}k_1\mathrm{d}k_2\mathrm{d}k_3$, $k_j=2\pi/L_j$ is the wave number, L_j is the length scale of the jth turbulence, and $\mathrm{i}=\sqrt{-1}$ is the unit of imagining number.

Based on the spectral analysis theory of stochastic process, the turbulence component $v_j(\mathbf{x},t)$ can be expressed as the following Fourier-Stieltjes integration formula (Shinozuka and Deodatis, 1996):

$$v_j(\mathbf{x},t)=\int_{R^3}\exp(\mathrm{i}\mathbf{k}\cdot\mathbf{x})\mathrm{d}Z_j(\mathbf{k},t) \quad (4)$$

where $\mathrm{d}Z_j(\mathbf{k},t)$'s are zero-mean incremental stochastic processes which satisfy the following conditions

$$\mathrm{E}\left[\mathrm{d}Z_j(\mathbf{k},t)\right]=0, \mathrm{d}Z_j(\mathbf{k},t)=\mathrm{d}Z_j^*(-\mathbf{k},t) \tag{5}$$

$$\mathrm{E}\left[\mathrm{d}Z_i(\mathbf{k}_1,t)\mathrm{d}Z_j^*(\mathbf{k}_2,t)\right]=\begin{cases} 0 & , \quad \mathbf{k}_1 \neq \mathbf{k}_2 \\ \Phi_{ij}(\mathbf{k},t)\mathrm{d}\mathbf{k}, & \mathbf{k}_1=\mathbf{k}_2=\mathbf{k} \end{cases} \tag{6}$$

In general, the turbulence wind field is a real-valued field, thus there exists $v_j(\mathbf{x},t)=v_j^*(\mathbf{x},t)$.

1.2. Taylor's frozen hypothesis

Considering that the turbulence component of atmospheric turbulence is an ergodic stochastic field, it thus satisfies Taylor's frozen hypothesis. The essence of Taylor's hypothesis is to replace the time extension of turbulence with the spatial extension (Simiu, 2019). Let $\tilde{v}_j(x_1,x_2,x_3)=v_j(x_1,x_2,x_3,0)$ denote the turbulence at the position (x_1, x_2, x_3), and at the time t=0. Taylor's hypothesis of frozen turbulence presumes that the fluctuations of the wind velocity at an observation point may be approximately considered as the effect of the convection of the field $\tilde{v}_j(x_1,x_2,x_3)$ with the mean wind taking placed velocity $V(x_3)$ without any local dispersion. Then, Taylor's hypothesis implies the functional relationship

$$v_j(x_1,x_2,x_3,t)=\tilde{v}_j(x_1-V(x_3)t,x_2,x_3) \tag{7}$$

It can be seen that the 4-D temporal-spatial stochastic field are reduced to a 3-D spatial stochastic field through Taylor's frozen hypothesis, which greatly reduce the calculation efforts of the numerical simulations.

1.3. Spectral tensor of isotropic homogenous field.

In section 1.1, the atmospheric turbulence components are expressed as Fourier-Stieltjes integration formulae. Once the spectral tensor of the turbulence field is determined, the 3-D turbulent wind field can be simulated through the spectral decomposition technique. In this paper, ignoring the shear effects, the atmospheric boundary layer turbulence field can thus be regarded as an isotropic homogeneous field.

Considering that the statistical correlation of the homogenous turbulent field is independent of spatial coordinates, we have

$$\frac{\partial R_{ij}(\mathbf{r})}{\partial r_j}=\frac{\partial E\left[v_i(\mathbf{x})v_j(\mathbf{x}+\mathbf{r})\right]}{\partial r_j}=0 \tag{8}$$

Correspondingly, the Fourier transform of Eq. (8) satisfy

$$\begin{aligned}\int_{-\infty}^{\infty}\int_{-\infty}^{\infty}\int_{-\infty}^{\infty}\frac{\partial R_{ij}(\mathbf{r})}{\partial r_j}\exp(-\mathrm{i}\mathbf{k}\cdot\mathbf{r})\mathrm{d}\mathbf{r} &= \\ \int_{-\infty}^{\infty}\int_{-\infty}^{\infty}\int_{-\infty}^{\infty}\frac{\partial}{\partial r_j}\left[R_{ij}(\mathbf{r})\exp(-\mathrm{i}\mathbf{k}\cdot\mathbf{r})\right]\mathrm{d}\mathbf{r} &- \\ \int_{-\infty}^{\infty}\int_{-\infty}^{\infty}\int_{-\infty}^{\infty}R_{ij}(\mathbf{r})\frac{\partial}{\partial r_j}\left[\exp(-\mathrm{i}\mathbf{k}\cdot\mathbf{r})\right]\mathrm{d}\mathbf{r}\end{aligned} \tag{9}$$

According to the physical properties of the spatial correlation function, we have $R_{i,j}(\pm\infty,r_2,r_3)=R_{i,j}(r_1,\pm\infty,r_3)=R_{i,j}(r_1,r_2,\pm\infty)=0$, thus the first term on the right hand side of Eq. (9) is zero. Then, considering Eq. (2), Eq. (9) can be rewritten as follows

$$\begin{aligned}&\int_{-\infty}^{\infty}\int_{-\infty}^{\infty}\int_{-\infty}^{\infty}\frac{\partial R_{ij}(\mathbf{r})}{\partial r_j}\exp(-\mathrm{i}\mathbf{k}\cdot\mathbf{r})\mathrm{d}\mathbf{r} \\ &=\mathrm{i}k_j\int_{-\infty}^{\infty}\int_{-\infty}^{\infty}\int_{-\infty}^{\infty}R_{ij}(\mathbf{r})\exp(-\mathrm{i}\mathbf{k}\cdot\mathbf{r})\mathrm{d}\mathbf{r} \\ &=\mathrm{i}k_j\Phi_{ij}(\mathbf{k})=0\end{aligned} \tag{10}$$

and

$$\int_{-\infty}^{\infty}\int_{-\infty}^{\infty}\int_{-\infty}^{\infty}\frac{\partial R_{ij}(\mathbf{r})}{\partial r_i}\exp(-\mathrm{i}\mathbf{k}\cdot\mathbf{r})\mathrm{d}\mathbf{r}=k_i\Phi_{ij}(\mathbf{k})=0 \tag{11}$$

For the isotropic homogenous turbulence field, the second order spectrum tensor is also isotropic, which can be expressed as follows (Zhang et al., 2005):

$$\Phi_{ij}(\mathbf{k})=F(k_m k_m)k_i k_j+G(k_m k_m)\delta_{ij} \tag{12}$$

Substituting Eq. (12) into Eq. (10) and Eq. (11), and the following relation can be derived

$$G(k_i k_i)=-F(k_i k_i)k^2 \tag{13}$$

where $k^2 = k_i k_i$ satisfy Einstein's summation convention. Thus Eq. (12) can be rewritten as follows:

$$\Phi_{ij}(\mathbf{k}) = F(k_i k_i)(k_i k_j - k^2 \delta_{ij}) \qquad (14)$$

Eq. (14) indicates that the energy spectrum of turbulent components is only dependent on the wave numbers for isotropic filed. In this view, the spherical symmetry characteristics, i.e., $\Phi_{ij}(\mathbf{k}) = -2k^2 F(k_i k_i)$, can be used to derive the spectrum tensor of the isotropic field. Integrating the turbulence kinetic energy over the wave number interval $(k, k+\mathrm{d}k)$, and thus the energy spectrum of turbulence can be obtained as

$$E(k) = -2\pi k^2 \Phi_{ii}(\mathbf{k}) = -4\pi k^4 F_{ii}(k_i k_i) \qquad (15)$$

Substituting Eq. (15) into Eq. (14), leads to the spectrum tensor of the isotropic homogenous turbulent field

$$\Phi_{ij}(\mathbf{k}) = \frac{E(k)}{4\pi k^4}(k^2 \delta_{ij} - k_i k_j) \qquad (16)$$

2. STOCHASTIC MODELING OF FROZEN TURBULENCE FIELD

2.1. Simulation formula

As mentioned in section 1, after determining the spectrum tensor function, the 3-D turbulence wind field can be simulated through the spectral decomposition technique. In order to perform numerical simulations of the turbulence field the position space and the wave number space are discretized. Then, the infinite integral in Eq. (4) is approximated by the following finite sum

$$\begin{aligned}
\tilde{v}_j(x_{l_1}, x_{l_2}, x_{l_3}) \approx 2\mathrm{Re}\sum_{n_1=1}^{N_1}\sum_{n_2=1}^{N_2}\sum_{n_3=1}^{N_3}\Big\{ & H_{jl}(k_{0,n_1}, k_{0,n_2}, k_{0,n_3}) \cdot \\
& \sqrt{\Delta k_0}\exp[\mathrm{i}\Theta_m^{(1)}(\mathbf{k}_0)]\exp[\mathrm{i}(x_{l_1}k_{0,n_1} + x_{l_2}k_{0,n_2} + x_{l_3}k_{0,n_3})] + \\
& H_{lm}(-k_{0,n_1}, k_{0,n_2}, k_{0,n_3})\sqrt{\Delta k_0}\exp[\mathrm{i}\Theta_m^{(2)}(\mathbf{k}_0)] \cdot \\
& \exp[\mathrm{i}(-x_{l_1}k_{0,n_1} + x_{l_2}k_{0,n_2} + x_{l_3}k_{0,n_3})] + \\
& H_{lm}(k_{0,n_1}, -k_{0,n_2}, k_{0,n_3})\sqrt{\Delta k_0}\exp[\mathrm{i}\Theta_m^{(3)}(\mathbf{k}_0)] \cdot \\
& \exp[\mathrm{i}(x_{l_1}k_{0,n_1} - x_{l_2}k_{0,n_2} + x_{l_3}k_{0,n_3})] + \\
& H_{lm}(k_{0,n_1}, k_{0,n_2}, -k_{0,n_3})\sqrt{\Delta k_0}\exp[\mathrm{i}\Theta_m^{(4)}(\mathbf{k}_0)] \cdot \\
& \exp[\mathrm{i}(x_{l_1}k_{0,n_1} + x_{l_2}k_{0,n_2} - x_{l_3}k_{0,n_3})]\Big\}
\end{aligned} \qquad (17)$$

where $H_{jl}(\mathbf{k}_0)$ is obtained through the spectrum decomposition of the spectral tensor, of which the analytical form is given as follows (Mann, 1998):

$$\mathbf{H}(\mathbf{k}_0) = \frac{E^{1/2}(k_0)}{(4\pi)^{1/2}k_0^2}\begin{pmatrix} 0 & k_{0,3} & -k_{0,2} \\ -k_{0,3} & 0 & k_{0,1} \\ k_{0,2} & -k_{0,1} & 0 \end{pmatrix} \qquad (18)$$

In Eq. (17), the following designations have been introduced

$$x_{l_i} = (l_i - 1)\Delta x_i, k_{0,n_i} = (n_i - i/3)\Delta k_{0,i}; (i = 1,2,3) \qquad (19)$$

And $\Theta_m^{(r)}(\mathbf{k}_0), (r = 1,2,3,4)$ in Eq. (17) are the identically distributed random variables uniformly distributed over the interval $[0, 2\pi]$. The corresponding normalized random variables, defined as $\bar{\Theta}_m^{(r)}(\mathbf{k}_0)$, satisfy the following conditions

$$\mathrm{E}\left[\bar{\Theta}_m^{(r)}(\mathbf{k}_0)\right] = 0, \mathrm{E}\left[\bar{\Theta}_m^{(r)}(\mathbf{k}_0)\bar{\Theta}_n^{(s)}(\mathbf{k}_0)\right] = \delta_{rs}\delta_{mn} \qquad (20)$$

The random variables $\Theta_m^{(r)}(\mathbf{k}_0)$ from all finite differential volumes of wave numbers constitute the basic variables of the turbulence model. Due to mutual independence of the random phases, the random field (17) will become approximately Gaussian due to the central limit theorem.

2.2. Random variables based on the evolutionary phase model

It is acknowledged from the above section that the number of random variables is $4\times3\times N_1\times N_2\times N_3$ if one wants to generate a 3-D turbulence wind field by using the Monte Carlo method. Theoretically, the efficiency of Monte Carlo methods is independent to the number of random variables. However, almost all of the methods for pseudo-random numbers generation confront the challenges of the high-dimensional random variables. In view of this, the evolutionary phase model (EPM) (Yan and Li, 2011) is adopted in this paper to generate the phase variables. By using the EPM, the phase variables can be expressed as follows

$$\Theta_m^{(r)}(\mathbf{k}_0)=\mathrm{mod}(|\mathbf{k}_0|\Delta\sigma_m(\mathbf{k}_0)T_e^{(r)},2\pi) \qquad (21)$$

where $\mathrm{mod}(\cdot)$ denotes the congruence symbol, $\Delta\sigma_m(\mathbf{k}_0)$ is the characteristic velocity for Fourier components of the turbulence in the *m*-direction with wave number vectors in $\Delta\mathbf{k}_0$, of which the expression is given as follows:

$$\Delta\sigma_m^2(\mathbf{k}_0)=\Phi_{mm}(\mathbf{k}_0)\Delta k_0 \qquad (22)$$

In Eq. (21), $T_e^{(r)}$ is the evolution time of the evolutionary phases which satisfy the following Gamma distribution

$$f_{T_e}(t_e)=t_e^{(\beta-1)}\frac{\mathrm{e}^{-t_e/\theta}}{\theta^\beta\Gamma(\beta)} \qquad (23)$$

where β and θ are the shape parameter and the scale parameter of the Gamma distribution, respectively. According to Li et al., (2013), $\beta=1.1$, $\theta=8.2\times10\wedge8$.

It can be seen that the number of random variables in Eq. (17) is greatly reduced to 4 after introducing the EPM, which significantly reduce the difficulty of random simulation for 3-D turbulent fields. More importantly, since the random variables are uniquely determined by the basic random variables, i.e., $T_e^{(r)}$, thus each representative point of $T_e^{(r)}$ can uniquely generate one representative time histories of the 3-D turbulent wind velocity.

2.3. FFT algorithm

The proposed scheme is readily to take the advantages of the three-dimensional FFT algorithm to reduce the computational effort for digitally generating sample processes. In conjunction with the FFT algorithm, Eq. (17) can be rewritten as

$$\begin{aligned}\tilde{v}_j(x_{l_1},x_{l_2},x_{l_3})=2\mathrm{Re}\Big[&\mathrm{FFT}_{k_{0,3}}\{\mathrm{FFT}_{k_{0,2}}[\mathrm{FFT}_{k_{0,1}}(G_j^1)]\}+\\&\mathrm{FFT}_{k_{0,3}}\{\mathrm{FFT}_{k_{0,2}}[\mathrm{iFFT}_{k_{0,1}}(G_j^2)]\}+\\&\mathrm{FFT}_{k_{0,3}}\{\mathrm{iFFT}_{k_{0,2}}[\mathrm{FFT}_{k_{0,1}}(G_j^3)]\}+\\&\mathrm{iFFT}_{k_{0,3}}\{\mathrm{FFT}_{k_{0,2}}[\mathrm{FFT}_{k_{0,1}}(G_j^4)]\}\Big]\end{aligned} \qquad (24)$$

where

$$\begin{cases}G_j^1(\mathbf{k}_0)=H_{jl}(k_{0,n_1},k_{0,n_2},k_{0,n_3})\sqrt{\Delta k_0}\exp[\mathrm{i}\Theta_m^{(1)}(\mathbf{k}_0)]\\G_j^2(\mathbf{k}_0)=H_{jl}(-k_{0,n_1},k_{0,n_2},k_{0,n_3})\sqrt{\Delta k_0}\exp[\mathrm{i}\Theta_m^{(2)}(\mathbf{k}_0)]\\G_j^3(\mathbf{k}_0)=H_{jl}(k_{0,n_1},-k_{0,n_2},k_{0,n_3})\sqrt{\Delta k_0}\exp[\mathrm{i}\Theta_m^{(3)}(\mathbf{k}_0)]\\G_j^4(\mathbf{k}_0)=H_{jl}(k_{0,n_1},k_{0,n_2},-k_{0,n_3})\sqrt{\Delta k_0}\exp[\mathrm{i}\Theta_m^{(4)}(\mathbf{k}_0)]\end{cases} \qquad (25)$$

The advantage of FFT algorithm lies in that the summation of cosine function with respect to wave number component could be omitted safely, leading to the considerable reduction of computational time of the numerical simulation.

3. NUMERICAL EXAMPLE

3.1. Simulation parameters

In order to illustrate the proposed approach, a numerical 3-D turbulence wind field for the 5-MW Hywind FOWT will be simulated in this section. The von Karman energy spectrum model is employed to calculate the spectrum tensor of the isotropic homogenous turbulent field, of which the expression is given as follows (Batchelor, 1953):

$$E(k_0)=\varepsilon\eta^{2/3}L^{5/3}\frac{(Lk_0)^4}{(1+(Lk_0)^2)^{17/6}} \qquad (26)$$

where ε is the Kolmogorov constant, η is the rate of viscous dissipation of specific turbulent kinetic energy.

According to the structural parameters of the FOWT, the 3-D spatial field frame based on the Taylor frozen hypothesis is shown in Figure 1. The corresponding wind field parameters of the numerical example are listed in Table 1.

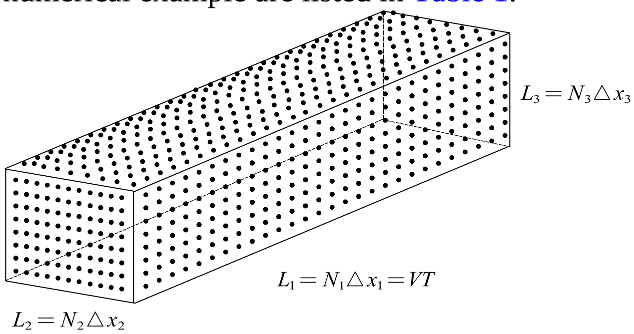

Figure 1: The 3-D spatial field frame of the Hywind FOWT.

Table 1: Wind field parameters of the numerical example

Parameters	Values
Time interval d*t* (s)	0.25
Mean wind speed at hub (m/s)	10
Along-wind spatial interval d*x* (m)	2.5
Simulation duration (s)	256
Characteristic length scale *L* (m)	28
Along-wind spatial length L_1 (m)	2560
Across-wind spatial length L_2 (m)	8*L*
Vertical-wind spatial length L_3 (m)	8*L*
Spatial discrete points N_1	1024
Spatial discrete points N_2	32
Spatial discrete points N_3	32
Number of representative points of random variables	100

3.2. Simulation results and discussions

As listed in Table 1, the number of representative points of the four dimensional elemental random variables, i.e., $T_e^{(r)}$, is 100, which indicates that 100 representative samples of the 3-D turbulence field will be generated. Figure 2 shows the representative sample of the turbulence component *u* on the rotational plane of the rotor, i.e., *xoz* plane. It can be seen that the turbulent eddies are very uniformly distributed on the two-dimensional plane of the rotor, and thus the homogeneity of the isotropic wind field are reflected by the proposed approach. Correspondingly, Figure 3 shows the representative time histories of the three turbulence components at the hub. It can be seen that the time-domain simulation results of the 3 turbulent components by the proposed approach have the typical stationarity and randomness of the turbulence wind speed processes.

Figure 4 shows the mean and standard deviation time histories of the simulated 3-D turbulence wind velocities by the proposed method at the hub and their target values. It can be seen that the mean value processes of the 3 turbulence components are zero, and the simulation results of both mean and standard deviation match pretty well with the target values. It should be noted that the standard deviation of the three turbulence components in Figure 4(b) are very close to each other, which is not consistent with the actual three-dimensional turbulence wind field in the atmospheric boundary layer, as discussed by Solari (2001) and Mann (1998). This is because that only the isotropic homogenous turbulence model was considered in this paper, and the shear effects, which results in the redistribution of turbulence kinetic energy between different turbulence components, are ignored.

Figure 5 shows the comparisons of the power spectral densities (PSDs) of the three turbulence components at one point between the simulation results and the target values. The target PSDs of the turbulences are given by Mann (1994). It can be seen that the simulated PSDs of different turbulence components are in good consistent with target values. Besides, one can find that the cross PSD between different turbulence components are zero, as shown in Figure 5(b), which indicates that there are no energy transforms between the different turbulence components, and this is determined by the physical properties of the isotropic turbulent field. The comparisons reveal that the proposed approach can reasonably simulate the isotropic homogenous turbulence wind field in both the time domain and the frequency domain.

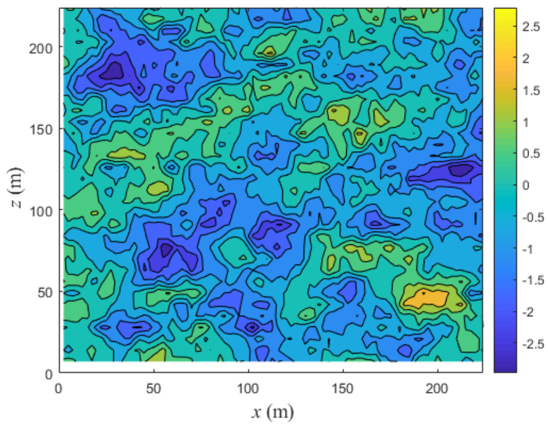

Figure 2: Representative sample of the turbulent wind field on the rotor plane.

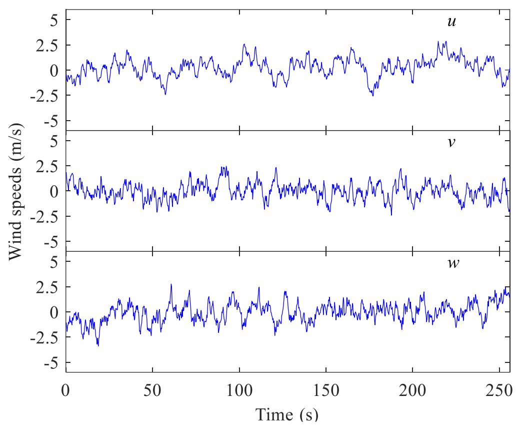

Figure 3: Representative time histories of the turbulent wind field at hub.

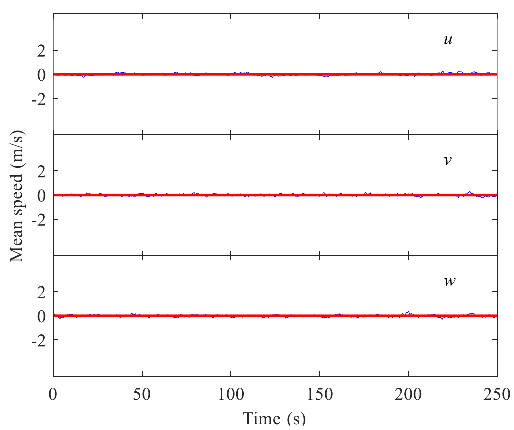

(a) Mean

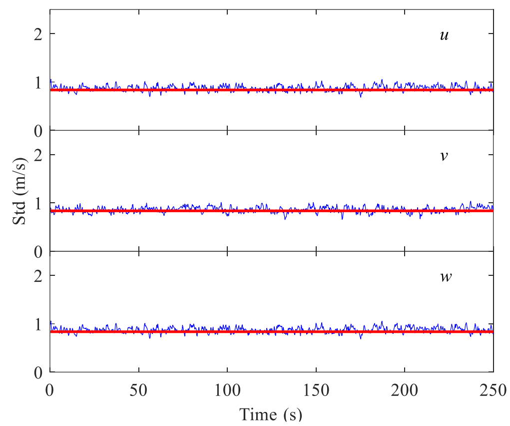

(b) Standard deviations

Figure 4: Mean and standard deviation of simulated turbulence component processes at hub.

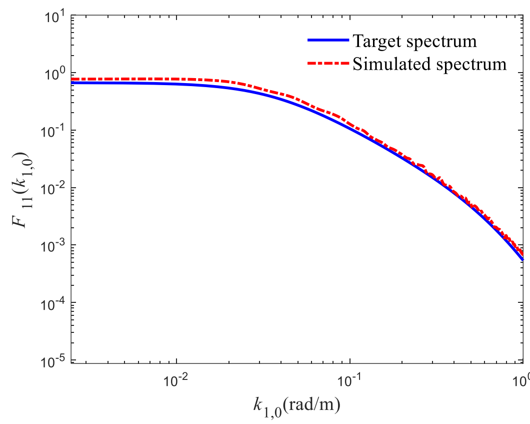

(a) Auto PSD of single point

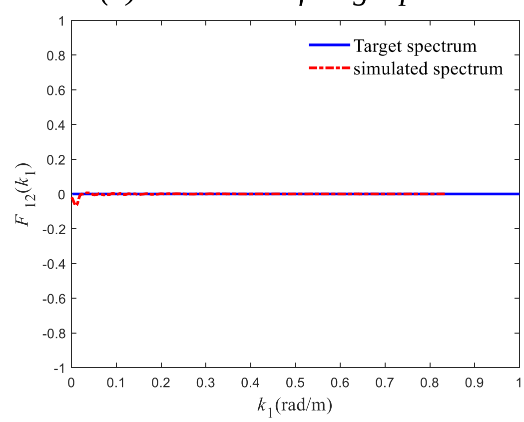

(b) Cross PSD of different turbulence components of single point

Figure 5: Comparisons of PSDs of different turbulence components at one point.

4. CONCLUSIONS

This paper proposed a physical modeling approach of 3-D turbulence wind field for FOWTs. In the proposed approach, Taylor's frozen hypothesis was used to convert the 4-D time-space turbulence field into the 3-D spatial field, and the isotropic turbulence model was adopted to derive the spectral tensor function of the turbulence. On this basis, the spectral decomposition technique was used to simulate the numerical wind field of FOWT, and the evolutionary phase model was introduced to reduce the number of random variables to 4. Finally, the three-dimensional FFT algorithm was adopted to enhance the efficiency of the numerical simulations.

The results of the numerical example of 3-D turbulence wind field of FOWT show that the representative sample of the simulation has the typical characteristics of the turbulence wind speed, and the statistical-moment-based comparisons reveal the effectiveness of the proposed approach in both the time domain and frequency domain for the simulation of the isotropic homogenous.

5. REFERENCES

Batchelor, G.K., (1953). The Theory of Homogeneous Turbulence. Cambridge University Press.

Chen, J., Song, Y., Peng, Y., Nielsen, S.R., Zhang, Z., (2020). An efficient rotational sampling method of wind fields for wind turbine blade fatigue analysis. Renewable Energy 146, 2170-2187.

Connell, J., (1981). Spectrum of wind speed fluctuations encountered by a rotating blade of a wind energy conversion system: observations and theory. Battelle Pacific Northwest Labs., Richland, WA (USA).

Hansen, M., (2015). Aerodynamics of Wind Turbines. Routledge.

Li, J., Peng, Y., Yan, Q., (2013). Modeling and simulation of fluctuating wind speeds using evolutionary phase spectrum. Probabilistic Engineering Mechanics 32, 48-55.

Mann, J., (1994). The spatial structure of neutral atmospheric surface-layer turbulence. Journal of Fluid Mechanics 273, 141-168.

Mann, J., (1998). Wind field simulation. Probabilistic Engineering Mechanics 13 (4), 269-282.

Veers, P.S., (1988). Three-dimensional wind simulation. Sandia National Labs., Albuquerque, NM (USA).

Shinozuka, M. and Deodatis, G., (1996). Simulation of multi-dimensional Gaussian stochastic fields by spectral representation. Applied Mechanical Review 49 (1), 29-53.

Simiu, E. and Yeo, D., (2019). Wind Effects on Structures, Modern Structural Design for Wind, 4 ed. John Wiley & Sons.

Solari, G. and Piccardo, G., (2001). Probabilistic 3-D turbulence modeling for gust buffeting of structures. Probabilistic Engineering Mechanics 16 (1), 73-86.

Sundar, R.M., Sullivan, J.P., (1983). Performance of wind turbines in a turbulent atmosphere. Solar energy 31 (6), 567-575.

Townsend, A., (1980). The Structure of Turbulent Shear Flow. Cambridge University Press.

Tubino, F. and Solari, G., (2005). Double proper orthogonal decomposition for representing and simulating turbulence fields. Journal of Engineering Mechanics 131 (12), 1302-1312.

Yan Q., and Li J., (2011). Evolutionary-phase-spectrum based simulation of fluctuating wind speed. Journal of Vibration and Shock 30 (9), 163-169.

Zhang Z., Cui G., Xu C., (2005). Theory and Modeling of Turbulence. Tsinghua University Press.